Global Properties of Nucleus-Nucleus Collisions III

8. 11. 2013 Rozhovory o kvark-gluonovém plazmatu

Jindřich Lidrych

Contents

- Gluon Saturation in A+A Collision
- Transverse phase space: equilibrium and the QGP state
- Bulk hadron transverse spectra and radial expansion flow

Gluon Saturation in A+A Collisions

- arises once the areal transverse parton density exceeds the resolution, leading to interfering QCD sub-amplitudes that do not reflect in the total cross section in a manner similar to the mere summation of seperate, resolved color charges

- idea of saturation are motivated by HERA deep inelastic scattering (DIS) date on the gluon distribution function

Gluon Saturation in A+A Collisions

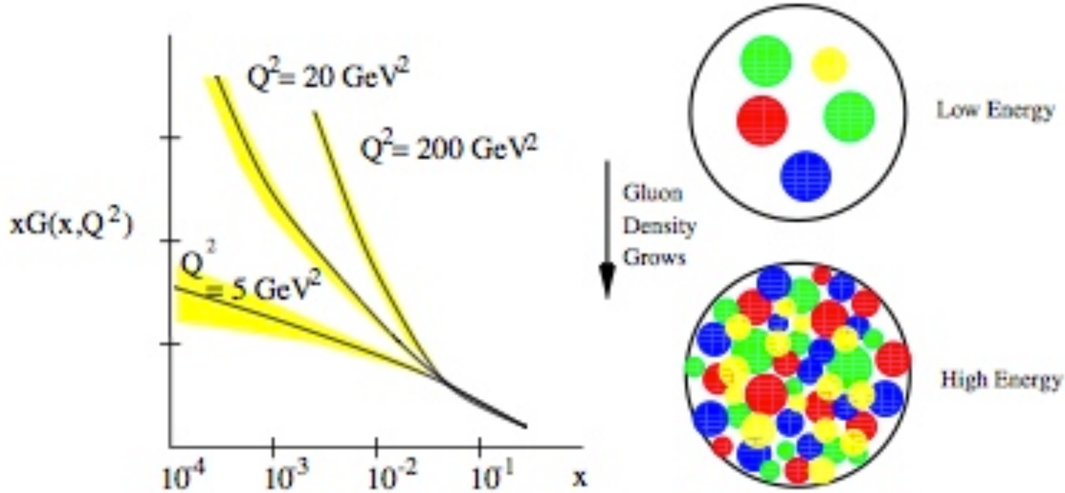

Fig. 16. (left) The HERA data for the gluon distribution function as a function of fractional momentum x and square momentum transfer Q^2 [61]. (right) Saturation of gluons in a hadron; a head on view as x decreases [64].

- Gluon distribution function $xG(x,Q^2) = \dfrac{dN^{gluon}}{dy}$

- Feynman x is defined as $x_F = \dfrac{p_L^*}{p_L^*(\max)} = \dfrac{2p_L^*}{\sqrt{s}}$

Gluon Saturation in A+A Collisions

• the rapidity of the potentially struck parton is defined as

$$y = y_{hadron} - \ln(1/x)$$

• the invariant rapidity distribution results as

$$dN/dy = xdN/dx = xG(x,Q^2)$$

• the dN/dy distribution of constituent partons of hadron is similar to the rapidity distribution of produced particles in hadron-hadron or A +A collisions

• apply the above conclusions: the rapidity density of potentially interacting partons grows with increasing distance from y_{proj} like $\Delta y \equiv y_{proj} - y = \ln(1/x)$

• at given Q^2 (<5GeV^2) the packing density at mid-rapidity increase as $\Delta y^{midrap} \approx \ln(\sqrt{s}/M) \approx \sqrt{s}/M$

Gluon Saturation in A+A Collisions

• for fixed x saturation occurs for transverse momenta below some critical $Q^2(x)$, $Q_s^2(x) = \alpha_s N_C \frac{1}{\pi R^2} \frac{dN}{dy}$

• as a consequence the saturation scale defines a critical areal resolution, with two different types of QCD scattering theory

• QCD scattering theory are limited => „Color Glass Condensate (CGC)“

• Q^2 - defines the effective transverse sampling area

• Q_s^2 - characteristic areal size at which satur. is expected to set in

• „geometric scaling“ - Q^2 / Q_s^2 - the characteristic behaviour of cross section

Gluon Saturation in A+A Collisions

- the virtual photo-absorption cross section in deep inelastic ep scattering with x<0,01
- plotted against Q^2 / Q_s^2, with

$$Q_s^2(x) \approx \left(\frac{x_0}{x}\right)^{\lambda} 1GeV^2 \text{ with } \lambda \cong 0{,}3\text{ , } x_0 \cong 10^{-4}$$

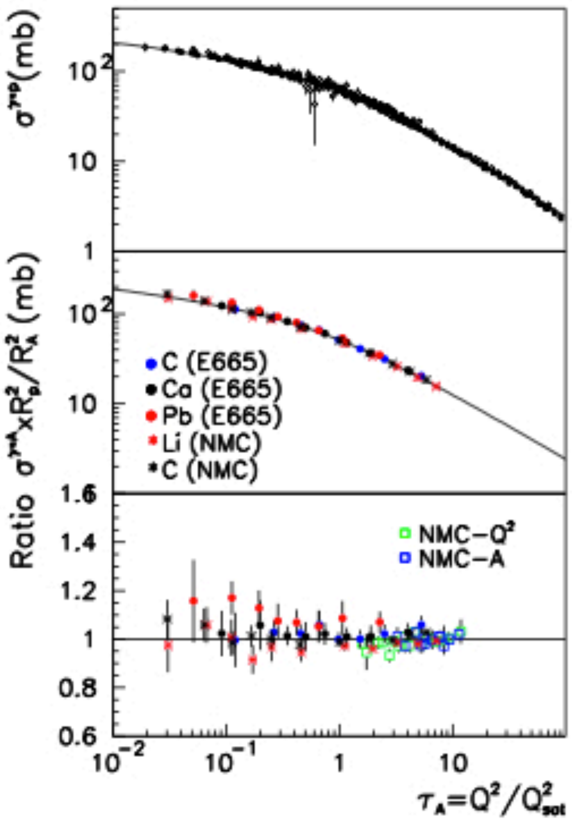

Fig. 17. (top) Geometric scaling of the virtual photo-absorption cross section $\sigma^{\gamma p}$ on protons; (middle) cross sections for nuclei normalized according to equation 94; (bottom) the ratio of $\sigma^{\gamma A}$ to a fit of $\sigma^{\gamma p}$ (see [53] for data reference).

Gluon Saturation in A+A Collisions

- Armesto, Salgado and Wiedemann for virtual photon-A interactions

$$Q_{s,A}^2 = Q_{s,p}^2 \left(\frac{A \pi R_p^2}{\pi R_A^2} \right)^{1/\delta}$$

- transforming these findings to the case of A+A collisions by

$$\frac{dN^{AA}}{dy}(y \approx 0) \propto Q_{s,A}^2(x) \pi R_A^2$$

$$\frac{1}{N_{part}} \frac{dN^{AA}}{dy}(y \approx 0) = N_0 \left(\sqrt{s}\right)^{\lambda} N_{part}^{\alpha}$$

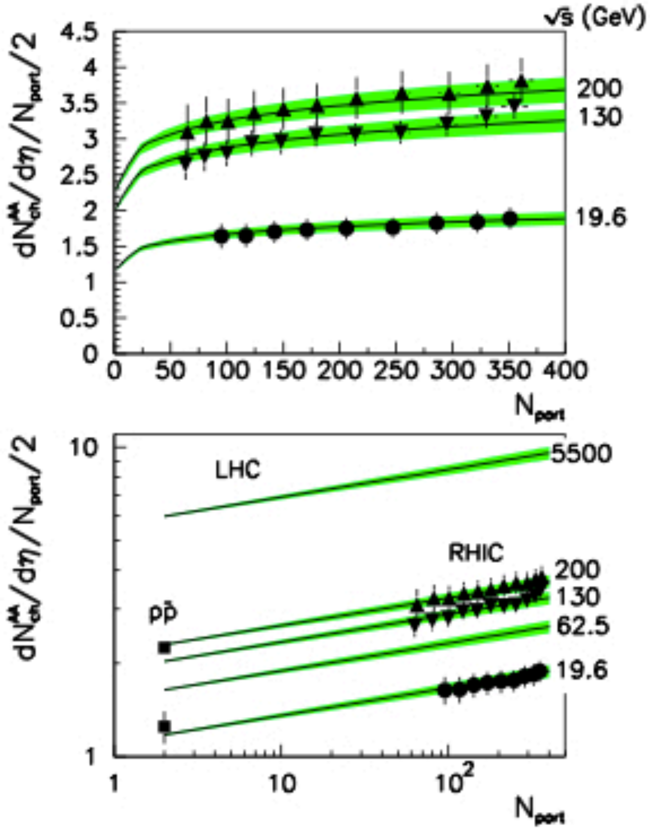

Fig. 18. Saturation model fit [53] applied to RHIC charged hadron multiplicity data at mid-rapidity normalized by number of participant pairs, at various energies [71]. Also shown is an extrapolation to $p\bar{p}$ data and a prediction for minimum bias Pb+Pb collisions at LHC energy, $\sqrt{s} = 5500\ GeV$.

Transverse phase space: equilibrium and the QGP state

- RHIC energy, the Au+Au collision, at a nuclear radius $R \approx A^{1/3} fm, \gamma \approx 100$
  - primordial interpenetration phase ends at time $\tau_0 \leq 0{,}15 \, fm/c$
    - this time scale is absent in e^+e^- annihilation at similar $\sqrt{s}$ where $\tau_0 \approx 0{,}1 \, fm/c$ marks the end of the primordial pQCD partonic shower evolution during which the initially $q\bar{q}$ created pair
  - in A+A collision this should be over 0,25fm/c
  - an aspect of equilibrium formation is observed in the relative production rates of the various created hadronic species -> „hadrochemical" equilibrum

Transverse phase space: equilibrium and the QGP state

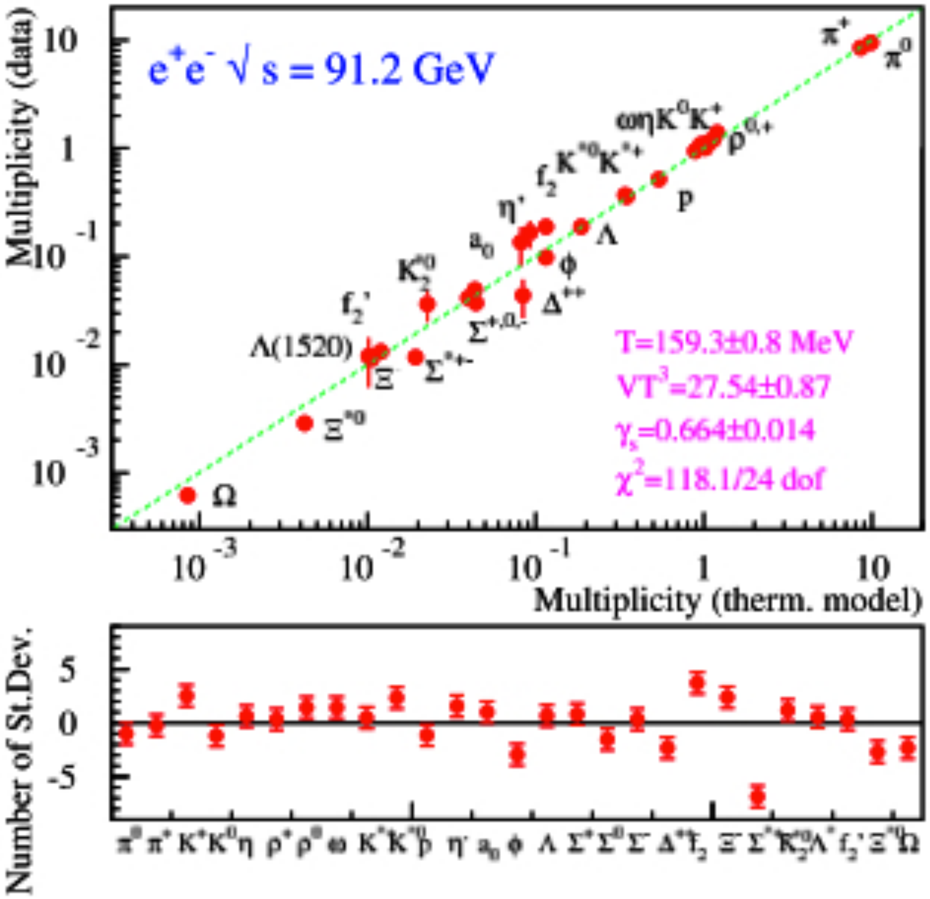

Fig. 19. Hadron multiplicities in LEP e^+e^- annihilation at $\sqrt{s} = 91.2\ GeV$ confronted with the predictions of the canonical statistical hadronization model [73].

Transverse phase space: equilibrium and the QGP state

• after τ_0 interacting system grows to twice the nuclear radius, system needs about $15\, fm/c$

• may create certain equilibrium properties that allow us to treat the contained particles and energy in term of thermodynamic phases of mater, such as a partonic QGP liquid, or a hadronic liquid or gas

• time scale is Lorentz dilated for partons with a large longitudinal momentum or rapidity -> slow particles are produced first toward the center of the collision region

• Bjorken „inside-out“ correlation is similar to the Hubble expansion pattern in cosmology

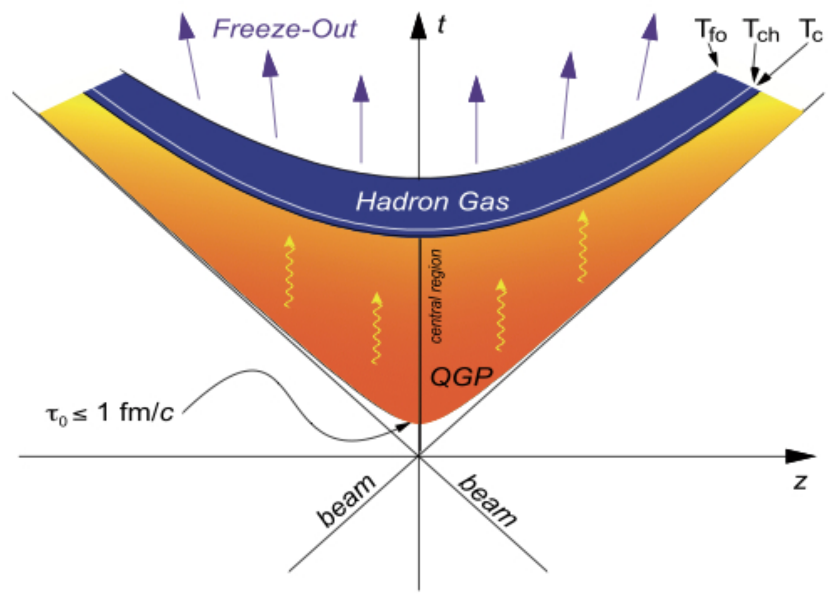

Fig. 2. Description of heavy-ion collisions in one space (z) and one time (t) dimension.

Transverse phase space: equilibrium and the QGP state

- for description of the primordial dynamics is used Bjork estimate of energy density $\varepsilon = \left(\frac{dN_h}{dy}\right)\left\langle E_h^T \right\rangle \left(\pi R_A^2 t_0\right)^{-1}$
- we need estimates both of the proper relaxation time scale –lattice QCD
- considerations suggest that a quark-gluon plasma state should be created early in the expansion dynamics at $\sqrt{s} = 200GeV$ at about $T = 300MeV$

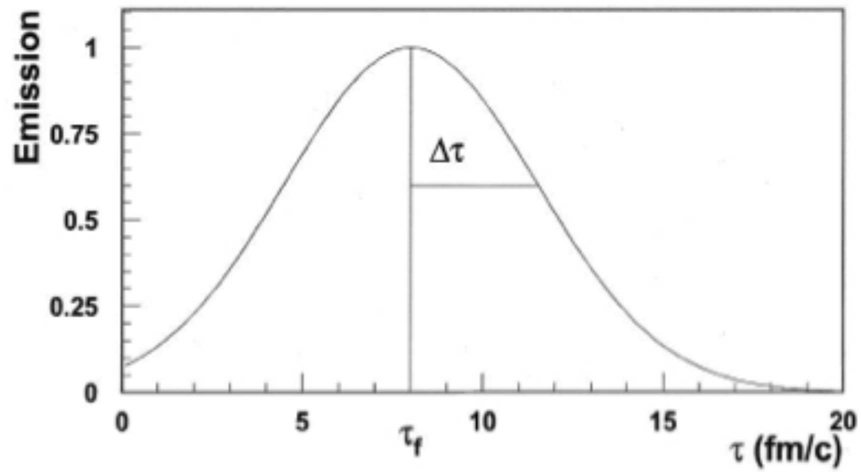

Fig. 20. Time profile of pion decoupling rate from the fireball in a central Pb+Pb collision, with $\tau = 0$ the end of the formation phase. Bose-Einstein correlation of $\pi^-\pi^-$ pairs yields an average Gaussian decoupling profile with $\tau_f = 8\ fm/c$ and duration of emission parameter $\Delta\tau = 4\ fm/c$ [76, 77].

Bulk hadron transverse spectra and radial expansion flow

- analyze bulk hadron transverse momentum spectra obtained at SPS and RHIC
- confronting the data with predictions of the hydrodynamical model
- central collision are selected to exploit the azimuthal symmetry of emission
- rewrite the invariant cross section for production of hadron species *i*

$$\frac{dN_i(b)}{p_T dp_T dy d\varphi_P} = \frac{1}{2\pi}\frac{dN_i(b)}{p_T dp_T dy}\left(1 + 2v_1^i\left(p_T b\right)\cos\varphi_P + 2v_2^i\left(p_T b\right)\cos(2\varphi_P) + \ldots\right)$$

Bulk hadron transverse spectra and radial expansion flow

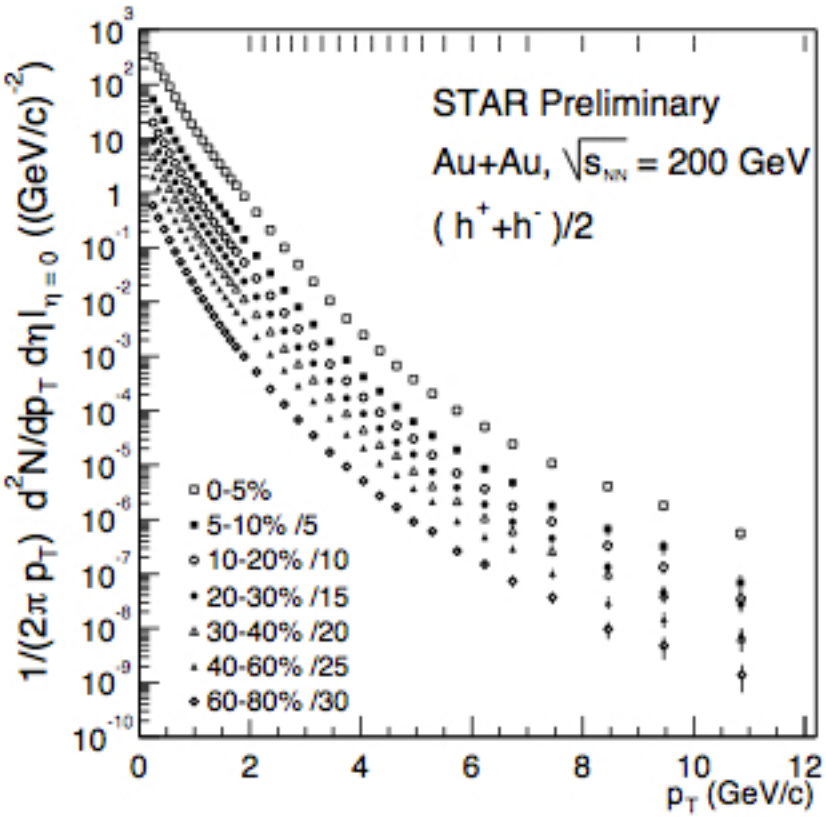

Fig. 21. Transverse momentum spectra of charged hadrons in Au+Au collisions at $\sqrt{s}$ = 200 GeV, in dependence of collision centrality [85] (offset as indicated), featuring transition from exponential to power law shape.

Bulk hadron transverse spectra and radial expansion flow

- transform to the transverse mass variable via $\frac{1}{2\pi}\frac{dN_i}{p_T dp_T dy} = \frac{1}{2\pi}\frac{dN_i}{m_T dm_T dy}$
- m_T distribution of various hadronic species „scaling“

$$\frac{1}{2\pi}\frac{dN_i}{m_T dm_T dy} = A_i \exp(-m_T^i / T)$$

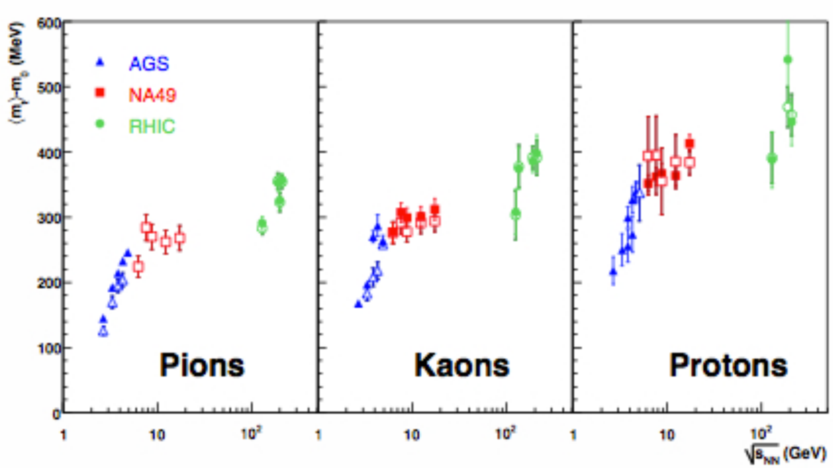

Fig. 22. The average transverse kinetic energy $\langle m_T \rangle - m_0$ for pions, kaons and protons vs. $\sqrt{s}$ in central Au+Au/Pb+Pb collisions [44]. Open symbols represent negative hadrons.

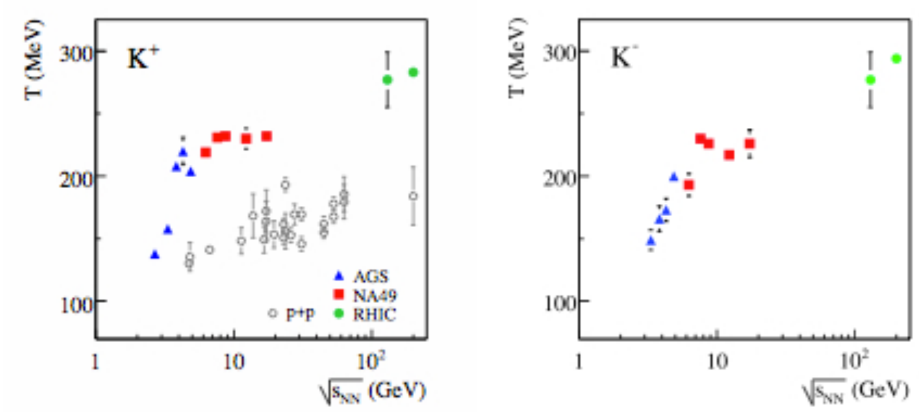

Fig. 23. The inverse slope parameter T of equation 103 for $K^+$and K^- transverse mass spectra at $p_T < 2\,GeV/c$ and mid-rapidity in central A+A, and in minimum bias p+p collisions [88].

Bulk hadron transverse spectra and radial expansion flow

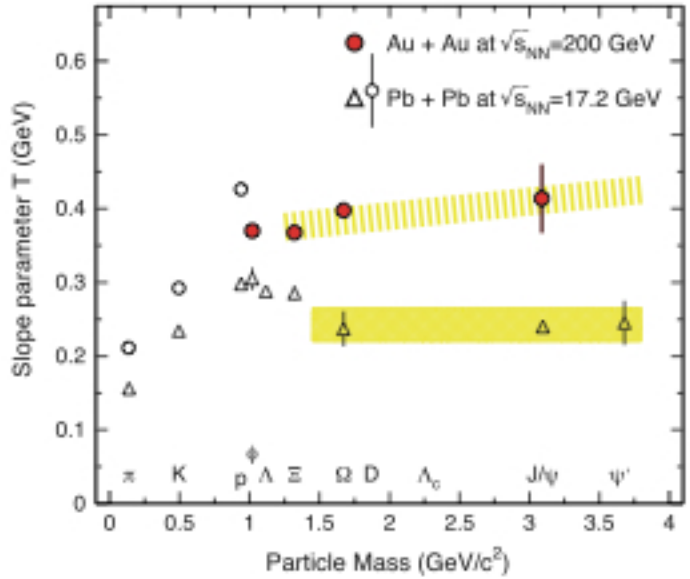

Fig. 24. Hadron slope parameters T at mid-rapidity as a function of mass. For Pb+Pb at $\sqrt{s} = 17.3\,GeV$ (triangles) and Au+Au at $\sqrt{s} = 200\,GeV$ (circles); from [92].

Bulk hadron transverse spectra and radial expansion flow

- hadronic expansion is known to proceed insentropically and we can expect $T = T_F + m_i \langle \beta_T \rangle^2 ,\ p_T \le 2GeV/c$

$$T = T_F \left(\frac{1 + \langle v_T \rangle}{1 - \langle v_T \rangle} \right)^{1/2} ,\ p_T >> m_i$$

$$\frac{dN_i}{m_T dm_T dy} = A_i m_T K_1 \left(\frac{m_T \cosh \rho}{T_F} \right) I_0 \left(\frac{p_T \sinh \rho}{T_F} \right)$$

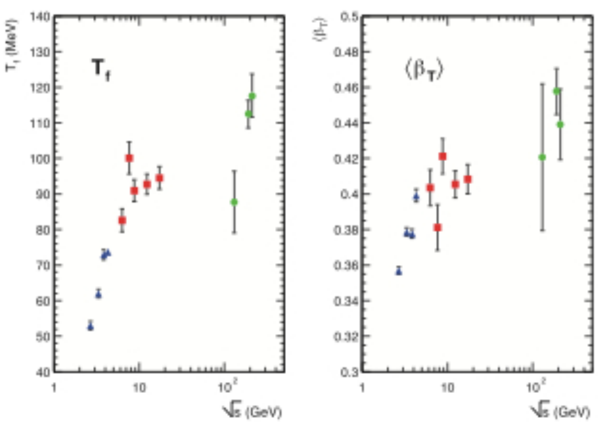

Fig. 25. Hadron decoupling temperature T_f, and average radial flow velocity $\langle \beta_T \rangle$ extracted from blast wave model (see equation 106) fits of m_T spectra vs. $\sqrt{s}$ [44].

- transverse mass spectrum of hadrons should contain the variable T_F at decoupling from the flow field and its $\langle \beta_T \rangle$, common to all hadron <-> the blast wave model developed as an approximation to the full hydrodynamic formalism

THE END

Thank you for your attention